Acoustic Sense & Avoid for UAV's

Anthony Finn & Stephen Franklin

Defence and Systems Institute (DASI)
University of South Australia
Mawson Lakes, SA 5095

anthony.finn@unisa.edu.au
stephen.franklin@unisa.edu.au

Abstract—**Based on successful results obtained from a laboratory prototype and real-world experiments, this paper discusses an innovative technique for providing small Unmanned Aerial Vehicles (UAVs) with 360 degree field of view sense and avoid capability. The proposed approach allows an aircraft equipped with appropriate acoustic sensors and processing to detect and accurately track other aircraft, manned or unmanned, in their proximity, determine whether or not they pose a threat, and, if necessary, take appropriate autonomous, quick-reaction measures to avoid them. The prototype is based on reliable, low-cost hardware that is platform independent, omni-directional, passive and draws little power. The technology is equally effective in day and night time conditions and also offers the prospect of retrofit to manned aircraft to provide them with a similar capacity to detect and avoid UAVs.**

I. Introduction

There is a general need for Uninhabited Aerial Vehicles (UAVs) to fly in civilian, uncontrolled airspace in a safe and economic fashion. In order to achieve this, they will probably need to meet requirements at an equivalent or higher level of safety comparable to the 'sense-and-avoid' requirements for manned aircraft (sense-and-avoid is the process of trying to detect obstacles in the path of the aircraft, determining whether or not they pose a threat, and, if necessary, taking measures to avoid them). There are a range of systems (e.g. TCAS, ADS-B) that partially satisfy these requirements, but they only aid in avoiding cooperative aircraft. Other technologies such as radar are likely to be of use due to their all weather capabilities, but weight, size, cost and power constraints mean that they are unlikely to be considered practical solutions for small-medium sized aircraft. Furthermore, current 'radar-on-a-chip' solutions lack the necessary detection, range and resolution performance.

Recent advances in the miniaturisation of high resolution electro-optic and infra-red sensor technology have combined with improvements in image processing algorithms and computing power to raise the possibility that computer vision techniques might be used to provide UAVs with a real time see-and-avoid capability against non-cooperative targets. However, such techniques are hampered by significant false alarm rates and cannot operate in all weather conditions, at night, or over 360 degree fields of view. Ground-based sensor systems are also of benefit, but introduce another level of integration complexity as they cannot be placed in many remote locations and struggle to detect small, slow-moving objects at long ranges with confidence.

The acoustic signal emitted by a propeller-driven aircraft consists of a strong narrowband tone superimposed onto a broadband random component [1]. The tone corresponds to the propeller passage frequency, which in the case of a turbo-prop aircraft is fixed (i.e. the source frequency is constant). Using a small array of microphones located onboard an aircraft and a combination of narrow and broad band processing techniques we may characterise the temporal variation of the received tone of an approaching aircraft and estimate its propeller blade rate (and hence type), together with its speed and the time and distance to the point of closest approach.

While clearly hostage to the propagation properties of sound in air and the closing speed of any approaching aircraft, the proof of concept demonstrations indicate effective detection ranges for reasonable aircraft velocities. The technique therefore potentially represents a useful aid to manned aircraft and/or UAV situational awareness. Furthermore, as only a small percentage of near misses and mid-air collisions occur head-on, with the bulk taking place from behind or the side and from above or below, typical closing velocities are often relatively modest and potential detection ranges correspondingly greater. The techniques examined thus far are particularly effective for rotary wing aircraft.

II. Basic Equipment & Setup

Three microphones were located on the vertices of an equilateral triangle, ostensibly onboard a UAV (for the Aerosonde UAV selected for trials this represented one in each wing and one in the tail); a fourth microphone was located approximately at the centre of the circle, but offset from the plane of the array by about 10cm (effectively on the upper or lower shell of the fuselage). A number of different noisy fixed and rotary wing model aircraft engines were then placed at the centre of this array to simulate the acoustic signature of the host UAV. The engine was run at full speed (~18,000rpm). The sensor array was located near to a local airport to simultaneously observe and record the signatures of the host UAV engine and fixed and rotary wing aircraft taking off and landing nearby. The output from the microphones was recorded at a sample rate of 44.1 kHz on a 4-channel, 24-bit, 110dB dynamic range DAQ.

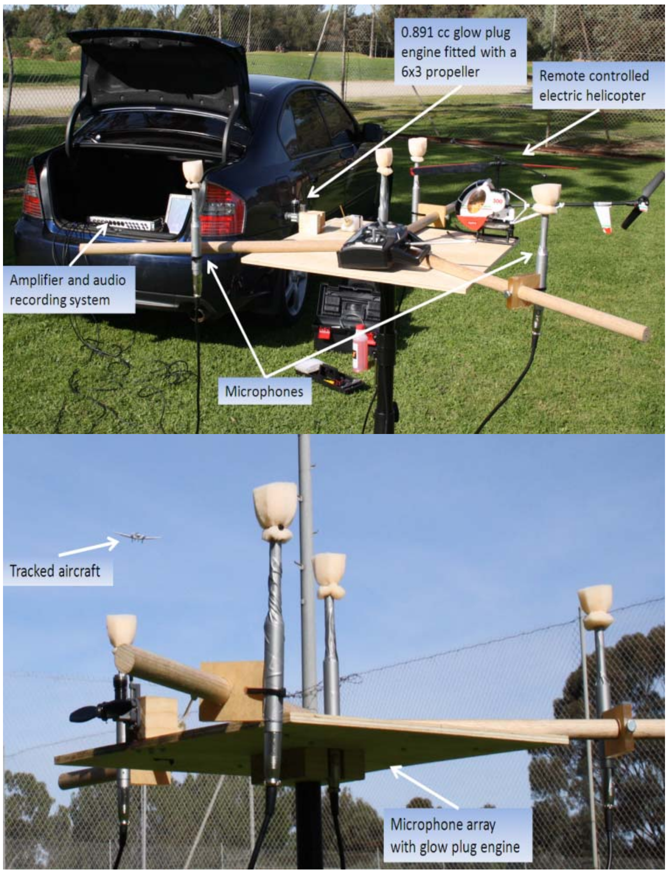

Figure 1: Prototype used to track acoustic signatures of an approaching aircraft

III. Detecting & Tracking Other Aircraft

As the array of three microphones is evenly distributed on a circle of radius, r, (equivalent to vertices on an equilateral triangle separated by a distance, $d = 1.75r$) and the outputs of each sensor sampled at 44.1 kHz the time difference of arrival (TDOA), τ_{n1}, of the signal at sensor pair (1, n) for $n = 2, 3$ may be determined by cross-correlating the outputs of the sensors on the sensing aircraft and then locating the peak of the cross-correlation function. As the range to any approaching aircraft is much greater than d the azimuth and elevation angles, Φ and θ, of the approaching aircraft can be determined from $\cos\emptyset = \frac{c}{d}\sqrt{X^2+Y^2}$ and $Tan\theta = \frac{Y}{X}$, where $X = \tau_{31} - \tau_{21}$ and $Y = \frac{1}{\sqrt{3}}(\tau_{31} - \tau_{21})$, where the value of the speed of sound, c, may be estimated from organic meteorological observations made by the UAV. The propagation path to the approaching aircraft can then be estimated by observing τ_{21} and τ_{31} and substituting these measurements into the above equations. Ultimately, accurate navigation data derived from the UAV's autopilot will need to be used to correct for any variation in TDOA resulting from the sensing aircraft's motion.

The broadband component of noise generated by the host aircraft is also correlated across the array, but arrives approximately 'in phase' on each of the three microphones. It may therefore effectively be excised as (in the ideal case) the cross-correlation peaks represent near-zero TDOA across the sensors. The component of the host UAV's acoustic signature generated by the blade rate of the propeller, is excised using the narrow band techniques described below.

For three sensors in a single plane, there is obviously an above/below ambiguity that must also be resolved. However, by placing the fourth sensor near (or preferably at) the centre of the circle, but out of the plane of the other three (on the outer shell of the UAV's fuselage), we can once again cross-correlate the time-series data. As the sampling rate of the DAQ is 50 kHz, as long as the vertical plane of separation is greater than ~1cm we may now resolve whether the second aircraft is approaching from above or below the UAV. TDOA peaks derived by differencing the spectrum on the fourth microphone with those obtained from the other three sensors in the array also permits discrimination between an approaching aircraft in the 'dead zone' created by the near-zero correlation peak described in the previous paragraph.

The angular trajectory of the approaching aircraft may be estimated by observing $\tau_{21}$and τ_{31} over time and calculating $\dot{\Phi}$ and $\dot{\theta}$. Using one of a number of non-linear least squares estimation techniques this information can then be combined with the time-varying Doppler shift in f_R to determine the relative motion of the two aircraft, the time to closest approach, and the miss-distance, along with the proportional navigation vector that provides optimal avoidance for the UAV. The vector effect of any wind on the apparent source of propagation must also be accounted for, but this is estimated from the onboard meteorological sensors.

If we assume a scenario in which the two aircraft are on a head-on collision course, that both aircraft must avoid each other by a minimum distance, r_{min}, and that the avoidance action is observed only by one of the aircraft, for a bank angle of φ initiated instantaneously by the evading aircraft, the turning radius will be $\frac{v_1^2}{g}\cot\emptyset$ [2]; in other words, the necessary detection warning time, $t_c = \sqrt{\frac{r_{min}}{g\tan\emptyset}}$. For a bank angle of 45deg and miss distance of 500ft (152.4m), in the absence of any processing requirements for detection, tracking, and risk assessment, and assuming the avoidance manoeuvre is initiated both autonomously and instantaneously, this corresponds to a warning of 3.9sec. For a closing velocity approaching 0.5c or more, this corresponds to about 600m, or – allowing for a few seconds of signal processing and track/risk assessment, about 1.5km. In other words, although increased detection ranges are desirable, despite the infancy of the approach, the techniques currently indicate that they are of general use in the avoidance of even higher velocity aircraft. Furthermore, only a small percentage of near misses and mid-air collisions occur head-on, with the bulk taking place either from behind or to the side from above or below. As a result, typical closing velocities will be significantly less than those indicated above so the likely timelines are correspondingly greater.

IV. NARROWBAND PROCESSING

A time-frequency signal analysis of own noise data showed strong narrowband tones superimposed onto a broadband random component, with most of the narrowband energy below 4 kHz. In order to examine this signature more closely the recorded data were down sampled by a factor of 5 prior to Fourier transformation. The data were processed in overlapping blocks, each containing 1024 samples, with 50% overlap between two consecutive blocks. A 2048-point fast Fourier transform (FFT) with a Hanning window was then used to compute the spectrum. The spectra of every 10 consecutive data blocks were then averaged to allow a time-frequency analysis of the first 15 harmonics. Very little narrowband energy appeared above 4 kHz.

Identifying the peaks and normalising the frequency by its harmonic number, n, resulted in a mean value of the fundamental frequency, f_0 = 259.2Hz, with 1σ standard deviation (normalised by harmonic number) of 4.2Hz. It was noted that the frequency and amplitude of each harmonic varied over time, but that over periods of about 5 sec any variations were linear. These highly distinct and readily identifiable narrowband harmonics can therefore be normalised and effectively excised from the sensing aircraft's signature [3].

As some harmonics are not observable by the receivers onboard the sensing aircraft due to wind noise, a similar technique for determining harmonic numbers is therefore used as a means of definitively and accurately determining f_0 for the approaching aircraft. This parameter, f_0, is then used in conjunction with τ_{21}, τ_{31}, $\dot{\Phi}$ and $\dot{\theta}$ to determine the time to collision and point of closest approach from the intersection of the derived hyperboloids.

Since the signature of approaching aircraft contain strong harmonically related tones, however, any cross-correlation calculations will contain ambiguous peaks. To overcome this problem, phase-transform pre-filtering, which uses only the cross-spectral phase information, may be used in the frequency domain implementation of the cross-correlation processing (i.e. we may ascribe similar Doppler bins to each approaching aircraft and use standard interferometric techniques to discriminate between the arrival directions of each). A sequence of time delay estimates may then be used to track the relevant peak of the cross-correlation function over time. Furthermore, if we have a library of acoustic signatures for aircraft types, we may also rely upon processing gain derived through the correlation of the observed and library signatures to further extend the detection range.

V. OTHER CONSIDERATIONS

As the majority of conflict situations occur near airports, where air traffic is densest, it is imperative that multiple aircraft can be spatially discriminated. As this is performed in the frequency domain (see previous section) the possibility exists that two aircraft can present on the same (Doppler-shifted) frequency simultaneously, thereby corrupting the interferometric phase determination of their angles of approach (i.e. the two aircraft will appear as one approaching from another direction). However, if the approaching aircraft is moving such that its relative velocity to the sensing aircraft, $v = |\dot{\tilde{\boldsymbol{x}}}|$, makes an angle, θ, between its direction of travel and the acoustic propagation path, the transmitted spectrum is represented by a dominant frequency, f_T, then the frequency received at the sensing aircraft,

$$f_R \cong f_T + \frac{f_T}{c}\left[\frac{(x_1-x_2)(\dot{x}_1-\dot{x}_2)+(y_1-y_2)(\dot{y}_1-\dot{y}_2)+(z_1-z_2)(\dot{z}_1-\dot{z}_2)}{\sqrt{(x_1-x_2)^2+(y_1-y_2)^2+(z_1-z_2)^2}}\right]$$

Consequently, unless identical aircraft are approaching at the same speeds on symmetric paths and the sensor aircraft is not subject to any rotational variation (which may be used to discriminate the spectra) the directional of arrival may be resolved.

While processing the Doppler from each sensor individually will be useful for multi-aircraft discrimination, it will generally be useful to reduce the temporal variation of the narrowband signals received by each sensor by averaging across all of them (after it has been suitably compensated for any significant rotational motion of the sensor aircraft). This will provide 'cleaner' data for Doppler processing.

In cases when the UAV is close to the ground and potentially susceptible to multi-path (for example during the early ground-test phases of this project), as we have accurate navigation data from the autopilot we will use this to calculate the maximum multipath delay, $h_r/c \cong 7$ms (where h_r is the height of the ground receiver) to discriminate the direct from the multi-path signals. The effects of multipath can, however, also cause constructive interference such that the detection ranges are extended. These effects will be examined and exploited, as will the effects of using electric propulsion aircraft to host the sensors.

In addition to the broadband acoustic energy and narrowband tones caused by the engine and the passage of the propeller, the sensing UAV signature will contain noise induced by the flow of air over the microphones. While not a limiting factor in the overall usefulness of the technique, a reduction in these broadband noise components would significantly increase the range at which approaching aircraft can be detected.

VI. EARLY TRIALS & RESULTS

Laboratory prototype technology has been developed (Figure 1) and the feasibility and performance envelope of the above approach is being examined against a range of both rotary and fixed wing civilian aircraft, including scenarios involving multiple aircraft, jet powered aircraft and aircraft with multiple engines. Both electric and fuel-engines have been used to generate the self-noise. Random broadband noise is added to simulate airflow over the microphones.

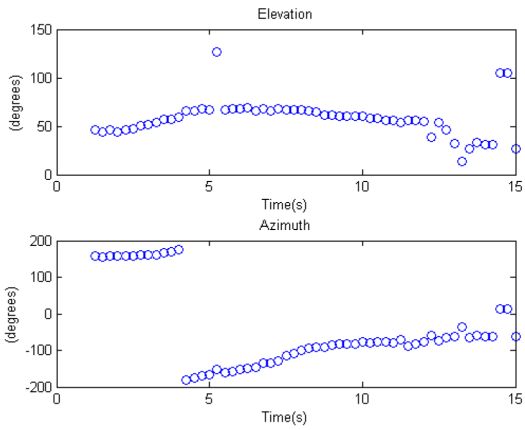

Figure 2: Azimuth and Elevation angles of the tracked aircraft while the electric helicopter was running at full throttle clamped to the microphone stand.

Figure 2 shows early results of azimuth and elevation tracks for an approaching aircraft in the presence of self noise (it shows only the central 15sec of the approaching aircraft's traverse). In this case, the sharp discontinuity in the lower figure is caused by a ±180deg 'phase flip' in the data. In this example, the self noise was generated by a (very noisy) electric helicopter clamped to the microphone stand and run at full throttle. (Note: although electric, the helicopter's acoustic signature is still very noisy. In fact, the peak amplitudes of the narrow band tones are similar in magnitude and closer together to those for the glow plug engine and the broadband energy is around 15-20dB higher).

Following determination of f_0 using the basic technique described above a non-linear least squares technique was used to determine the velocity of the approaching aircraft and the range and time to Closest Point of Approach (CPA) from the TDOA observations. The velocity of the aircraft was estimated to be 53.1 m/s (191.3 km/h) and the range at CPA 285.5m. The aircraft was tracked for a duration of ~50 sec which corresponds to a distance of about ±1.5km either side of CPA. When only observations prior to CPA were used, the predictions of the velocity and time to CPA were 218.3km/hr and 414m, respectively. This improved if data very close to CPA was used (i.e. < 3sec).

VII. FUTURE WORK

Work has now commenced on combining the narrow and broadband processing techniques with adaptive signal excision strategies to minimise and excise the effects of self-generated noise. Early results indicate significantly extended the detection ranges. Constraints are being applied to the range/time to CPA calculations and these too show considerable improvement.

The performance envelope of the technique is to be examined in a series of real world trials. These experiments comprise ground-based observations and flight trials that allow demonstration and characterisation of the technique in realistic conditions. The acoustic signatures of a range of manned and unmanned aircraft will also be accurately captured so that the narrow and broad band signal processing techniques can be refined and stress-tested against a variety of manned aircraft. An adjustable 2-D array of microphones will be integrated into the UAV wings to determine any temporal/spatial signal coherence (and hence optimal sensor separation) to maximise effectiveness of the adaptive cancellation techniques. Finally, the acoustic impact of environmental effects such as rain impacting the UAV will also be characterised.

ACKNOWLEDGEMENTS

We would like to thank Aerosonde/AAI Pty Ltd for their ongoing support and collaboration and Dr. Romeo Marian at the School of Advanced Manufacturing & Mechanical Engineering, UniSA for his help with the glow plug engines. We would also like to thank Yogesh Kalegowda for his assistance with the field measurements.

REFERENCES

[1] B.G. Ferguson & K.W. Lo, Turbo-prop and rotary-wing aircraft flight parameter estimation using both narrow-band and broadband passive acoustic signal processing methods, J. Acoustic Society America, Vol. 108, No. 4, October 2000

[2] Geyer, C. S. Singh, L. Chamberlain, Avoiding Collisions between Aircraft, Technical Report, Carnegie Mellon University, CMU-RI-TR-08-03, January 2008

[3] K.W. Lo & B.G. Ferguson, Tactical unmanned aerial vehicle localisation using ground-based acoustic sensors, Proceedings Intelligent Sensor, Sensor Networks & Information Processing Conference 2004, Melbourne, December 2004

[4] B.G. Ferguson, DSTO, Private Communication, 2010

[5] S. Rydergard, Obstacle Detection in See-And-Avid Systems for UAVs, TRITA-NA-E04013, Master's Thesis, Royal Institute of Technology, Stockholm, 2004

[6] H. Fujishima, R. Teo & A. Finn, Project Careful: Collision Avoidance for Multi-UAV Operations (Literature Survey)

[7] E. Tijs et al, Hear-and-Avoid for Micro UAVs, Proc. IMAV 2010, Germany, June 2010